J Nanostruct 11(4): 684-697, Autumn 2021

RESEARCH PAPER

Cellulose Nanocrystal (CNC) Synthesis: An AFM Study

Nasrin Shahmiri[1], Nahid Hassanzadeh Nemati[1], Ahmad Ramazani Saadatabadi[1,2], Massoud Seifi[3]*

[1]*Department of Biomedical Engineering, Science and Research Branch, Islamic Azad University, Tehran, Iran*
[2]*Department of Chemical & Petroleum Engineering, Sharif University of Technology, Tehran, Iran.*
[3]*Department of Orthodontics, Dental School, Shahid Beheshti University of Medical Sciences, Tehran, Iran*

ARTICLE INFO

Article History:
Received 08 May 2021
Accepted 09 September 2021
Published 01 October 2021

Keywords:
Acid hydrolysis
Atomic Force Microscopy
Cellulose nanocrystals
Filter paper
Morphology
Particle size

ABSTRACT

Cellulose nanocrystals (CNCs) are charged nanoparticles with a high aspect ratio derived from the most common biological polymer, cellulose. Acid hydrolysis is one of the most common methods for CNC production. Whatman #1 filter paper was hydrolyzed by sulfuric acid and characterized by AFM in this research to examine the morphology and size distribution of CNCs. One drop of CNC suspension was air-dried on microscope cover glass to be analyzed by AFM with non-contact mode. The CNC dimensions were determined by measuring individual and isolated particles (n=88) via Nanosurf Easyscan2 software. The measurement data was analyzed by Excel statistically. Synthesized CNCs were ellipsoidal with the length, height, and aspect ratio of 219.87 ± 42.12, 6.25 ± 2.27, and 41.17 ± 21.70 nm, respectively. Although the length and height of the produced CNCs were in acceptable range, but the width of CNCs was an overestimation and it was not reliable, mostly due to AFM tip broadening effect. Particle size measurement of CNCs is a challenging process because of their rapid aggregation and rod shape. Although hydrolysis parameters are influential on the final shape and size of CNCs, but it is necessary to optimize and maximize the quality of sample preparation and AFM adjustment to obtain the size of CNCs with the most accuracy and reliability. The CNC dimensions were determined by AFM are slightly different in the literature but height (thickness) is the most reliable one based on this experiment. Further studies are required to standardize CNC size measurement by AFM.

How to cite this article
Shahmiri N., Hassanzadeh Nemati N., Ramazani SaadatabadiA., Seifi M. Cellulose Nanocrystal (CNC) Synthesis: An AFM Study. J Nanostruct, 2021; 11(4): 684-697. DOI: 10.22052/JNS.2021.04.007

INTRODUCTION

Cellulose is the most common biological polymer found in the walls of all cell plants [1]. Cellulose nanocrystals (CNCs) are charged nanoparticles and derived from cellulose resources [2]. CNCs are approximately 3-5 nm in width and 50-500 nm in length. So, they have a high aspect ratio. CNCs are also ~100% cellulose and highly crystalline (54-88%) [3]. They also have unique properties such as high elastic modulus, dimensional stability, outstanding reinforcement potential, and transparency [4], and can be utilized in many fields like biomedical, wastewater treatment, energy, electronics, food engineering, and cosmetics [5]. CNCs can be produced by various methods such as acid hydrolysis, mechanical treatment, oxidation method, enzymatic hydrolysis, ionic liquid treatment, subcritical water hydrolysis, and combined processes [6], but among them, acid hydrolysis is one of the most popular methods for CNC production [7]. Acid hydrolysis dissolves the amorphous regions of cellulose chains, and the

* *Corresponding Author Email: nahid_hasanzadeh@yahoo.com*

short-crystalline particles will remain [8].

Among various aspects of CNC characterization, size and shape determination is an important challenge. The tendency of CNCs for making large and tightly packed agglomerations is a major limitation for the measurement of average particle size [9]. Particle size shows the quality of CNC suspension, but the direct observation of nanoparticles is a challenge and high-resolution direct imaging is required. In fact, particle size variability depends on the sample preparation conditions and the measurement techniques. The aspect ratio of CNCs determines the percolation threshold, a critical parameter to control mechanical properties in nanocomposites [10]. Nanocellulose widths can be estimated by microscopy (e.g., atomic force microscopy (AFM), scanning electron microscopy (SEM), and transmission electron microscopy (TEM)) and small-angle X-ray scattering. Some researchers utilize Laser Diffraction Analyzer for size measurements of CNCs. But this method is based on spherical shape particles, then size distributions should be considered relative as CNCs are rod shape [11, 12]. Dynamic Light Scattering (DLS) also provides an equivalent spherical hydrodynamic diameter and an intensity weighted distribution whereas microscopy gives a number weighted distribution. Furthermore, only individual CNCs are included in the AFM size analysis while any aggregates are included in the DLS size measurement [13-15]. Aggregates are a challenge during the size determination of CNCs. The pH of the CNC samples is drastically decreased during acid hydrolysis, causing a reduction in the charge density of the CNC particles, resulting in the formation of bundles and aggregates. It is unlikely that all of these aggregates can be redispersed completely, when the pH is readjusted [8]. The preparation of CNC samples with minimum agglomeration is useful for size study and assessing the impact of CNC dimensions on its properties [16]. Although, the most frequently utilized methods for CNC size analysis are TEM and AFM, either alone or in combination [14], but Chen et al. [16] showed that even by fractionation of CNC samples, there was a higher proportion of CNC clusters in TEM images in comparison with AFM ones, maybe due to the TEM deposition and staining process. AFM is less costly than TEM and provides accurate thickness values [14]. AFM characterization is a convenient, high resolution method for measuring CNC dimension. This technique does not require complicated sample preparation and can provide high quality images [9]. Dimension study of CNCs is ongoing and researchers use various methods, but AFM is still on the top shelf.

This study has been conducted to explain the acid hydrolysis process for the production of high-quality CNCs by details and examine the morphology and dimensions of produced CNCs based on Atomic Force Microscopy (AFM) analysis.

MATERIALS AND METHODS

Materials

Whatman #1 filter paper (Qualitative, 7cm, England), Whatman #541 hardened ashless filter paper (9 cm, pore size 22 µm, England), Sulfuric acid (H_2SO_4 95-97%, Merck, Germany), Dialysis tubing membrane (43 mm, MWCO 12-14 kDa, Sigma-Aldrich, Germany), pH-indicator strips (pH 0-14 Universal indicator, Merck, Germany), Acetone (CH_3COCH_3 99.5% purity, Asiapajohesh Co, Iran), Ethyl Alcohol (C_2H_5OH 96% v/v, Nasr Alcohol Co, Iran), Hydrogen peroxide (H_2O_2 3%, Kimiagartoos Co, Iran), Double distilled water (ddH_2O, Nabet Co, Iran), Microscope cover glass (18×18 mm, 0.13-0.17 mm thickness, Sail Brand, China) (All chemicals were used without further purification).

CNC Synthesis

CNCs were prepared through an acid hydrolysis process based on previous studies [17-27] as illustrated in Fig. 1. First, Whatman #1 filter paper (5gr) was chopped into small pieces of approximately 1 cm by 4 cm and milled with a coffee grinder (Moulinex, AR1044, ～50-60 HZ, China) with 2 sharp blades for 15 seconds [Ignition hazard]. Then, the ground paper was oven (Memmert, Germany) dried at 105°C for about 5 hours to remove moisture. After that, it was added to preheated sulfuric acid (100 ml, 64 wt%) in a beaker gradually, while it was stirring mechanically (～ 100 rpm) for 60 minutes at 45 °C on the heater (Heidolph, MR 3001 K, Germany) until a dull yellow solution was formed. The acid-to-paper ratio was 20:1 mL/g. During the hydrolysis process, some hydroxyl groups from the cellulose crystal surface are replaced by negatively charged sulfate groups, inducing repulsive electrostatic interactions between the nanocrystals that are responsible for the colloidal stability of the nanocrystal suspension [28]. The hydrolysis reaction was quenched with

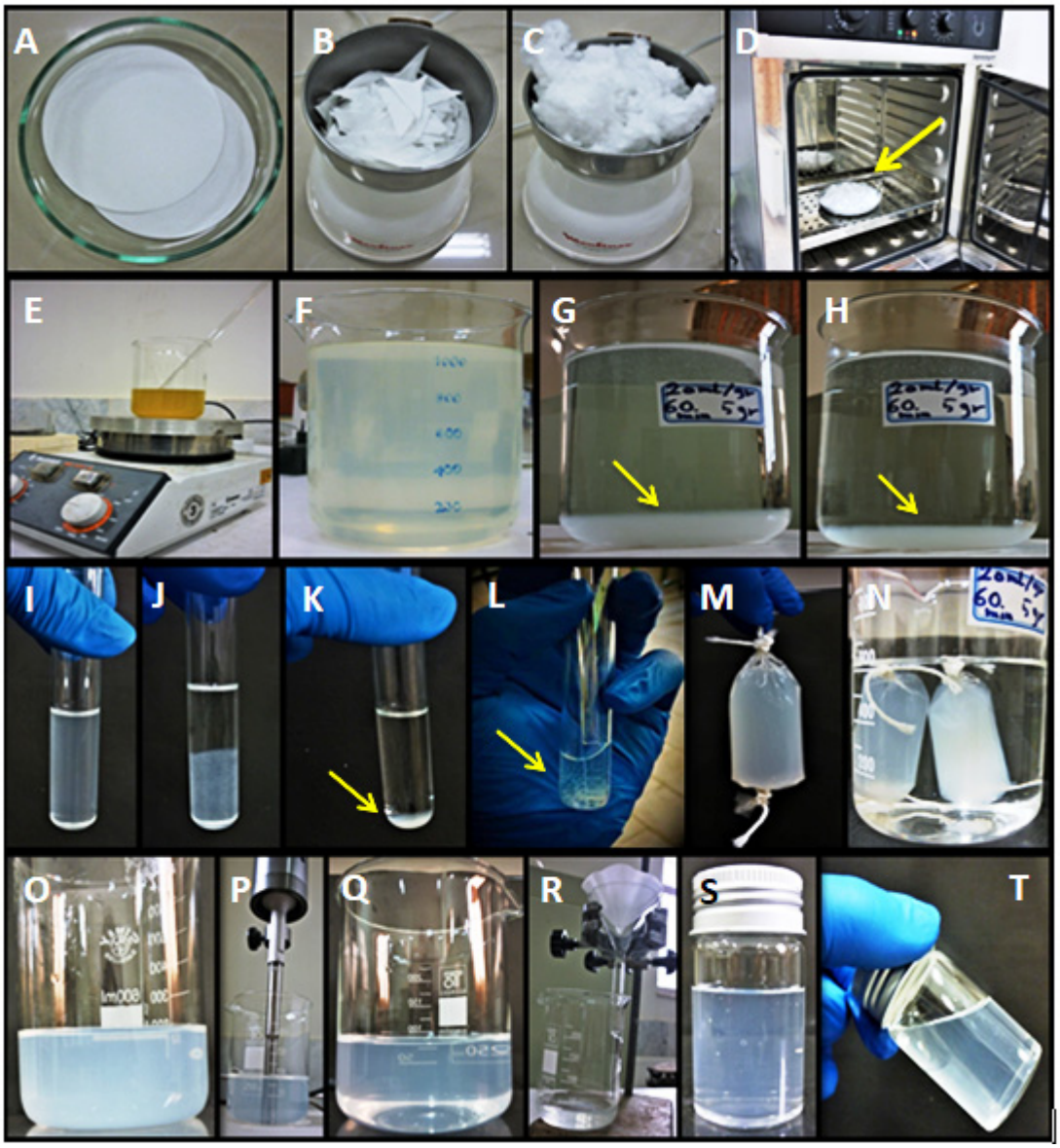

Fig. 1. Summary of CNC production. A) Whatman #1 filter paper B) Chopped filter paper in coffee grinder C) Ground filter paper D) Oven drying of ground filter paper E) Dull yellow slurry after acid hydrolysis F) Quenching of hydrolysis process with 10-fold cold water G) Settlement of CNC dispersion after 1 day H) Settlement after 4 days I) Redispersing CNCs in ddH_2O J) Separation of CNCs from acid after 5 min centrifugation K) CNC dispersion at the bottom of the tube after 30 min centrifugation L) Mechanical agitation of CNC pellets with a glass rod in fresh ddH_2O M)Filling dialysis tube with CNC suspension N) Dialysis tubes in ddH_2O O) Blur CNC suspension after dialysis process P) Probe sonication Q) Clear CNC suspension after sonication R) Filtration with Whatman #541 filter paper S, T) Final CNC slurry

10-fold cold ddH_2O (3 °C), and the solution was allowed to settle for 4 days. After settling, the clear supernatant was decanted and the resultant white slurry was centrifuged (Jouan, B 3.11, France) at 4100 rpm for 30 min. Following centrifugation, the clear supernatant was discarded again and the thick white pellet redispersed in ddH_2O by mechanical agitation to remove all soluble cellulose materials. The resulting CNCs were dialyzed against ddH_2O until the pH of dialysate remained constant (~4.5) and the conductivity remained below 5 µS/cm (~ 0.9 µS/cm) (Inolab Cond level 2, WTW, TetraCon 325, Germany). The dialysate was replaced with fresh ddH_2O daily

during the dialysis process. The dialysis stage was performed to remove excess acid, low molecular weight carbohydrates formed during hydrolysis, and other water-soluble impurities [29]. Then CNC suspension was probe sonicated for 10 min at 60% amplitude continuously with a 9.5 mm diameter tip (Ivymen, CY-500, Homogeneizador, Spain) to achieve colloidal cellulose particles. The sonicated CNC suspension was filtered via Whatman #541 ashless filter paper to remove large cellulosic particles, contaminants, and metal particles that might release from the sonication tip. The concentration of filtered CNC suspension was 0.096 wt% and stored at + 4 °C. (Except the temperatures mentioned in text specifically, other procedures were performed in ambient conditions)

Atomic Force Microscopy (AFM)

Nanosurf Easyscan 2 (Firmware version 3.1.0.4, Software version 2.2.1.16, Switzerland) was used for the determination of the size and morphology of the CNCs in this work. AFM tip radius was ~ 10 nm. Two images were obtained at a resolution of 512×512 pixels. The vibration frequency was 162.82 kHz. The vibration amplitude, excitation amplitude, cantilever type, head type, and setpoint were 0.1 V, 0.69 V, Tap190AI-G, EZ2-FlexAFM, and 50%, respectively. Imaging was performed with non-contact and phase contrast mode at room temperature in the air. Primary CNC suspension was diluted to approximately 0.001 wt% with ddH_2O and probe sonicated before deposition on the substrate (continuous, 9.5 mm diameter tip, 60% amplitude, 10 min) to reduce the number of aggregates. The microscope cover glass was utilized as substrate for drop-casting of diluted CNC. The substrate was cleaned to remove contamination and prepare a hydrophilic surface before drop-casting: first with detergent and tap water, then with acetone, ethyl alcohol, hydrogen peroxide, and finally with ddH_2O. A 0.3 ml drop of the diluted suspension was deposited on the glass surface with an approximate area of 1.5 cm^2 and allowed to dry in the air under ambient conditions for 4 hours to remove the water. The CNC film sample was placed in a polystyrene Petri dish for 3 days at room temperature before testing. Then the film was analyzed by AFM. Scans of 10 × 10 μm^2 and 5 × 5 μm^2 were performed to analyze the dimensions of CNCs. The size distribution was determined first by measuring 88 clear distinguishable particles with AFM (Nanosurf Easyscan2 version 2.2.1.16) software and then analyzed with Excel statistically. The length and width of CNCs were measured by drawing lines through the longitudinal and transverse axis of the crystal. The height was measured by transverse cross-sectioning of the crystal. The significant level of aggregation makes it impractical to use an automated analysis approach [30].

RESULTS AND DISCUSSIONS

Whatman #1 filter paper was used to extract CNCs in this study as it is manufactured from high-quality cotton linters with a minimum alpha-cellulose content of 98% [31]. Fig. 2 is an AFM topography image and Fig. 3 is an amplitude image of CNCs that prove the presence of cellulose nanocrystals. The average length, width, height, and aspect ratio of produced CNCs were 219.87 ± 42.12 nm, 138.80 ± 19.64 nm, 6.25 ± 2.27 nm, and 41.17 ± 21.70, respectively. The aspect ratio was calculated by dividing the length (the longest axis) of each crystal into the height (the shortest axis) of the crystal based on other studies [32]. Moreover, the AFM was used with a non-contact mode, so the aspect ratio was estimated as length/height [33]. CNC size measurement was performed via topography polynomial fit images. In fact, AFM images were flattened by polynomial fit (Nanosurf Easyscan 2 software) before the measurement. CNC films were also flat on the glass substrate with root mean square roughness (Rq) over a 5 × 5 µm and 10 × 10 µm area of 3.98 nm and 7.64 nm, respectively.

AFM results proved that CNCs have a cylindrical and rod-like structure with an ellipsoidal cross-section as the length and height of the CNCs were not the same. The length and width of all 88 particles were larger than the height which shows that the face of particles with the largest area was oriented to the glass surface makes the CNCs flatter and ribbon-like on the substrate. The obtained length and height values of the CNCs in this study are consistent with the values reported by previous studies [34, 35], regardless of the cellulose source. It means the CNCs that specifically derived from Whatman #1 filter paper were almost shorter and much thinner in the other studies. For example, Pakzad et al. [36] utilized Whatman #1 filter paper as a cellulose source, and reported the length, diameter, and aspect ratio of CNCs as 166±34 nm, 5.9±1 nm, and 28.7, respectively. On

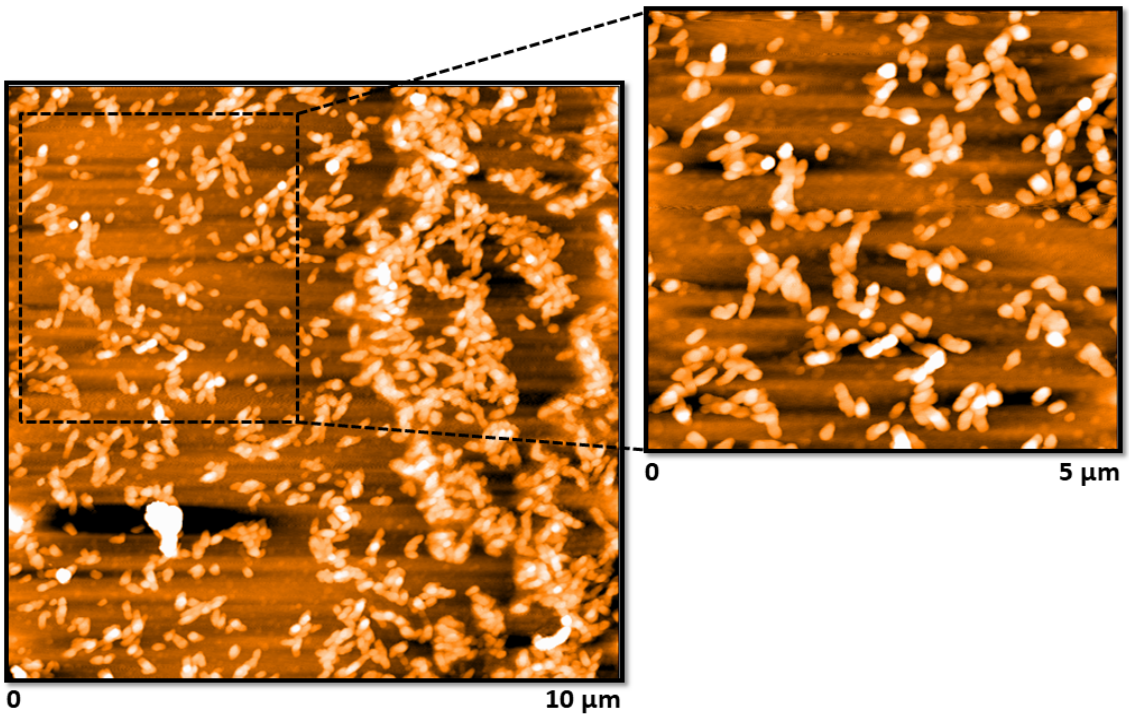

Fig. 2. AFM topography polynomial fit image of CNC.

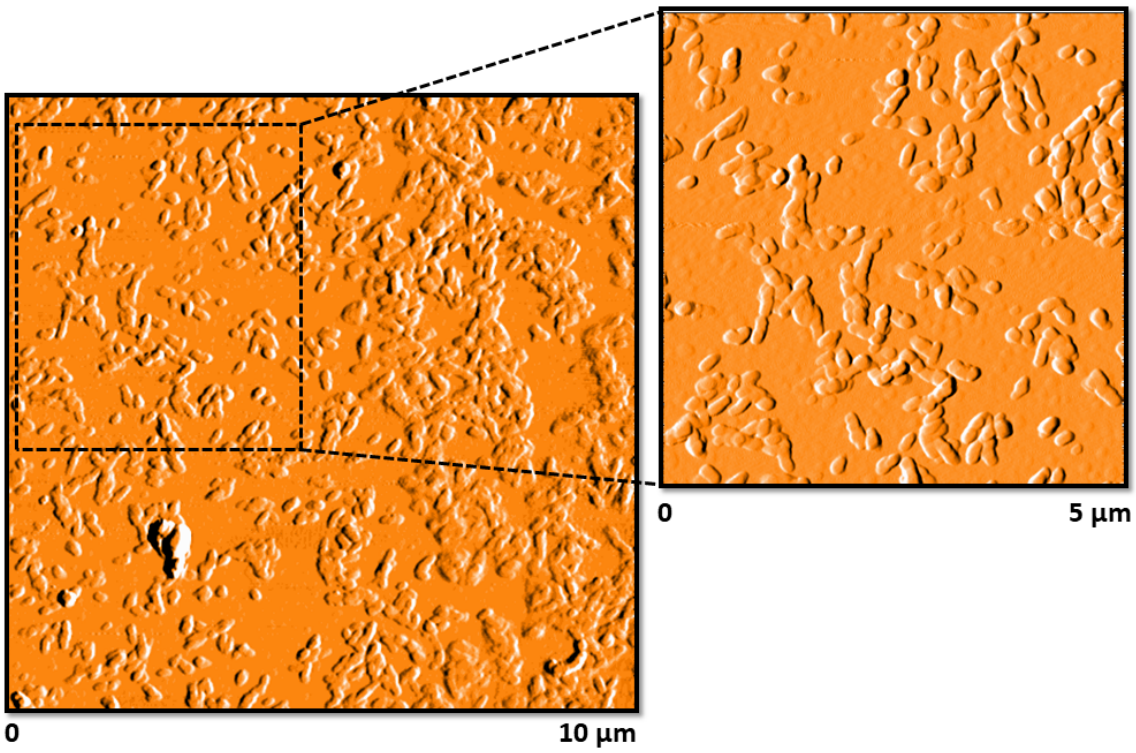

Fig. 3. AFM amplitude polynomial fit (left) and amplitude derived data (right) image of CNC.

Table 1. Dimensions of cellulose nanocrystals from various cellulose sources

Cellulose source	Length (nm)	Width (nm)	Height (nm)	Aspect ratio	Method	Reference
Cotton (Whatman Filters, grade 20 Chr)	195 ± 35	22 ± 3	6 ± 0.2	NR	SANS	[63]
Cotton (Whatman 541)	93.7 ± 31.6	21.2 ± 5.5	7.2 ± 3.0	13 (L/H)	AFM (AFM software)	[41]
Cotton powder (Whatman cellulose filter aid)	130 ± 63	20.4 ± 7.8	6.8 ± 3.3	6.6 ± 2.5 (L/W) 3.4 ± 1.3 (W/H)	AFM (Gwyddion 2.17)	[29]
office waste paper	238 ± 72	33 ± 5	5 ± 2	NR	AFM (Nanoscope software)	[34]
Bleached kraft eucalyptus wood pulp	240 ± 52	15.1 ± 1.4	3.8 ± 0.9	16 (L/W)	TEM (length, width, Image J) AFM (height)	[58]
Rice by-products	191.2	97.2	11.0	NR	AFM (AFM software)	[15]
Switchgrass	148 ± 42.1	21 ± 4.3	3.9 ± 1.3	39 (L/H)	AFM (AFM software)	[33]
CNF (Microfibrillated cellulose)	471.25 ± 150.12	8.56 ± 6.44		55.1 ± 20.4 (L/W)	TEM (Image J)	[39]
MCC	201 ± 12	16.4 ± 0.1	8 ± 2	13 (L/W)	TEM (length, width, Nano Measurer software) AFM (thickness, Nanoscope Analysis software)	[53]
Bamboo	100 ± 28	8 ± 3	4.5 ± 0.9	22 (L/H)	TEM (length, width, Image J) AFM (height, Gwyddion)	[40]

SANS (small-angle neutron scattering), TEM (transmission electron microscopy), AFM (atomic force microscopy), CNF (cellulose nanofibers), MCC (microcrystalline cellulose), NR (not reported), L (length), W (width), H (height)

the other hand, Annamalai et al. [37] reported the length, diameter, and aspect ratio of CNCs that were extracted from Whatman #1 filter paper as 365±80 nm, 34.5±6.1 nm, and 10.5±0.4. It is also worth mentioning that, Pakzad et al. [36] utilized AFM with contact mode to measure CNC dimensions but Annamalai et al. [37] measured CNC dimensions by TEM and ImageJ software. It shows that TEM has the potential to overestimate CNC dimensions. Because both mentioned studies used Whatman #1 filter paper as cellulose source and synthesized CNCs by sulfuric acid hydrolysis, but CNCs were longer and wider in Annamalai [37] study in comparison with Pakzad [36].

Rahimi Kord Sofla et al. [38] extracted CNC from sugarcane bagasse and measured the dimensions by TEM and Gatan digital micrograph software. They reported the length, diameter, and aspect ratio of CNCs as 160-400 nm, 20-30 nm, and 11, respectively. Pakzad et al. [36] also extracted CNC from wood MCC (Microcrystalline Cellulose), measured the size of CNC by AFM (contact mode), and reported the length, diameter, and aspect ratio of the CNCs as 310±45 nm, 4.2±1.2 nm, and 74. Different sources of cellulose that are used for CNC extraction [34] and different size analysis methods might affect the final reported dimensions of CNCs (Table 1).

The obtained aspect ratio (41.17 ± 21.70) in the present study is in agreement with the literature [33, 39]. The high value of aspect ratio proves the potential of produced CNCs as reinforcing agents in nanocomposites. Aspect ratio plays a major role in phenomena like the self-organization of CNCs into chiral nematic liquid crystal phases or the percolation threshold that is a key parameter governing mechanical properties [40]. Researchers reported different aspect ratios for CNCs (Table 1). This can be due to the wide polydispersity of CNCs in length and width. Besides, researchers may calculate the aspect ratio in different ways such as length/width, length/height or width/height, thus the results will be different.

The mean height of CNCs was calculated 6.25 ± 2.27 nm that is similar to previous studies. Urena-Benavides et al. [29] prepared CNCs from Whatman cellulose filter aid (cotton powder) with the average height of 6.8 ± 3.3 nm. Wu et al. [41] extracted cotton CNCs from Whatman #541 filter paper with the average height of 7.2 ± 3 nm. In contrast, the length and especially the width of synthesized CNCs were larger than mentioned studies (Table 1). There are some reasons for this difference that is discussed further in subsequent paragraphs.

Hydrolysis conditions and parameters are one of the important factors that influence CNC dimensions. Jakubek et al. [42] also confirmed that CNCs' size heterogeneity is more attributable to the initial hydrolysis process. The nature

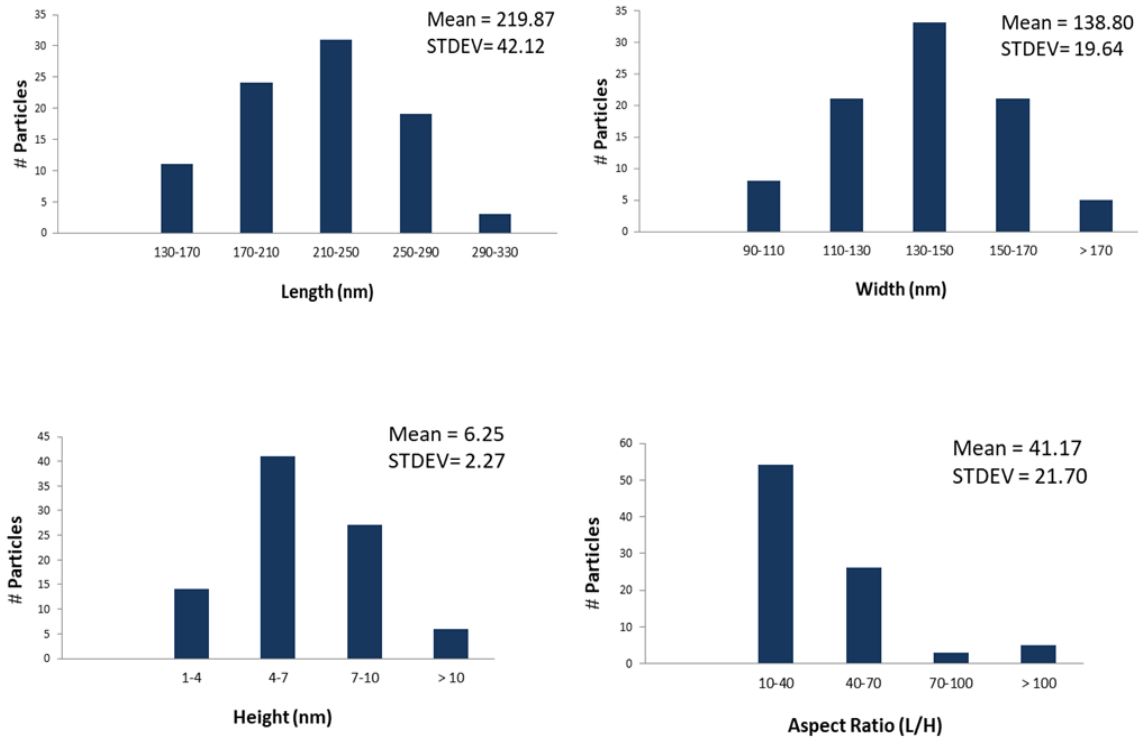

Fig. 4. Size distribution histograms of the cellulose nanocrystals (STDEV= Standard Deviation)

cellulose consists of ordered crystalline regions and amorphous regions. The principle of CNCs preparation is to dissolve amorphous regions in cellulose chains of nanofibers by acid hydrolysis and release the arranged crystalline regions that are rod-shaped, nano-sized particles; in fact, acid depolymerize cellulose and interchain hydrogen bonds in crystalline area increase [43-45]. Insufficient hydrolysis reaction leaves amorphous remnants at both ends of crystal and the CNCs become much longer.

The size histograms of the produced CNCs show broad distributions that can be justified by the large standard deviations (Fig. 4). This is a common phenomenon among cellulose nanocrystals according to Beck-Candanedo et al. [46], but monodispersion of nanoparticles makes them more appropriate to be utilized as reinforcing agents in comparison with polydispersion. The polydispersity of CNCs in length is not mainly due to the primary cellulose source utilized for CNC synthesis. In fact, the length of the CNCs strongly depends on the hydrolysis parameters [40].

Grinding is also important before the acid hydrolysis process. Kontturi et al. [47] dried pulp before grinding. That's why ground filter paper was dried to remove moisture in the present study. Tian et al. [48] showed specific surface area increase after grinding. It simply means that there will be a more accessible surface for fiber-acid reactions as shown in Fig. 5. It seems that grinding time must be enhanced in our study to facilitate hydrolysis, because Tian et al. [48] ground dissolving pulp at least for 30 seconds. Moreover, Tian et al. [48] utilized an Erlenmeyer flask for the acid hydrolysis process but a beaker was used for hydrolysis of filter paper in this research. Furthermore, stirring was not performed with constant rpm. It was variable somewhat between 80-100 rpm. Hydrolysis details might affect the final shape and size of the synthesized CNCs.

Gicequel et al. [49] showed that sonication can decrease the length of CNCs from 217 ± 42 to 150 ± 30 nm, but the height remained constant before and after sonication (10 ± 5 nm). So it was assumed at first that the high value of length and width of CNCs in this research might be due to insufficient sonication energy and duration but it was ruled out based on Jakubek et al. [42] study. They reported CNC samples sonicated with varying total energies, show similar size distributions for individual particles, although the

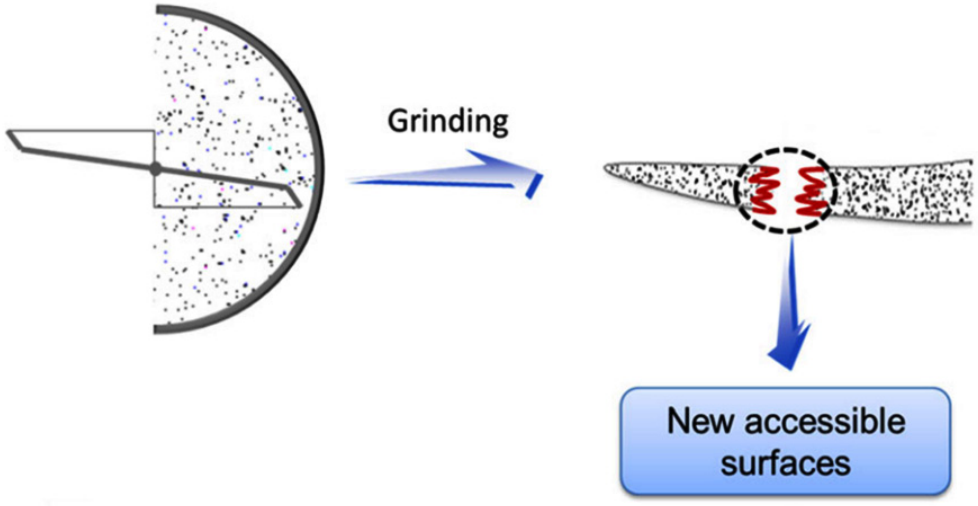

Fig. 5. The proposed effect of grinding on the fiber morphology. Adapted from [48].

number of clusters/image decreases with applied sonication energy. They also suggested that the individual particles comprising the agglomerates have a similar size distribution to the individual suspended particles [42].

It is claimed that AFM tip radius affects width measurements of CNCs [46]. AFM tip radius (Nanosurf Easyscan 2) was about 10 nm that is close to the size of CNCs, so the original size of nanoparticles during imaging might be affected and seems broader. Moreover, the tip radius has effect on the magnitude of tip broadening in the AFM images of CNCs. Navarro [14] found that the CNCs appeared broader and less anisometric in the image acquired with the tip with the largest nominal radius (< 15 nm) than in the image acquired with the tip with the smallest nominal radius (< 5 nm).

Urena-Benavides et al. [29] reported that for all CNC particles measured in their experiment, the width was always larger (on average 3.4 times larger) than the height, so they concluded that it would be inaccurate to assume that both dimensions (width & height) are equal. Leng [9] also mentioned that height of CNC does not equal the width. Because of this reason, all three dimensions including length, width, and height were measured for all 88 CNC particles in this work and the width of each particle was larger than the height. Fig. 6 shows the length, width, and longitudinal/transverse cross-section of an individual CNC. It is obvious that even longitudinal and transverse cross-section of CNC does not necessarily produce the same height. Kontturri et al. [47] and Beck-Candanedo et al. [46] reported that the actual width of CNCs in AFM images is unreliable because of the finite tip dimensions but the height measurement is accurate and is not subject to peak broadening artifacts. Furthermore, the CNC is assumed to be cylindrical in shape, so the height of the CNC can be taken equivalent to the width, to compensate for image widening due to the tip-particle convolution. AFM values are anticipated to be an overestimate due to tip convolution effects. Sample-tip convolution causes artifacts that can increase the width of CNCs. This overestimation of CNC dimensions due to tip broadening effects is unavoidable and causes an error in the length measurements, too [42, 46, 50]. So, some CNC researchers only report two dimensions as length-width or length-height and they consider the height as the same as width or vice versa. It seems that the height of CNCs is the most reliable dimension of cellulose nanocrystals that is reported in the literature as there is little difference among different researches.

Bushell et al. [30] also claimed that the variability between laboratories is larger for length than for height and attributed this variability to the challenges with the selection of individual particles, for example multiple aggregated particles might be analyzed as individual particles.

The method that is used for AFM sample preparation can also affect the nanocrystal length [34]. The diluted CNC must be filtered before deposition on a substrate according to Beck-

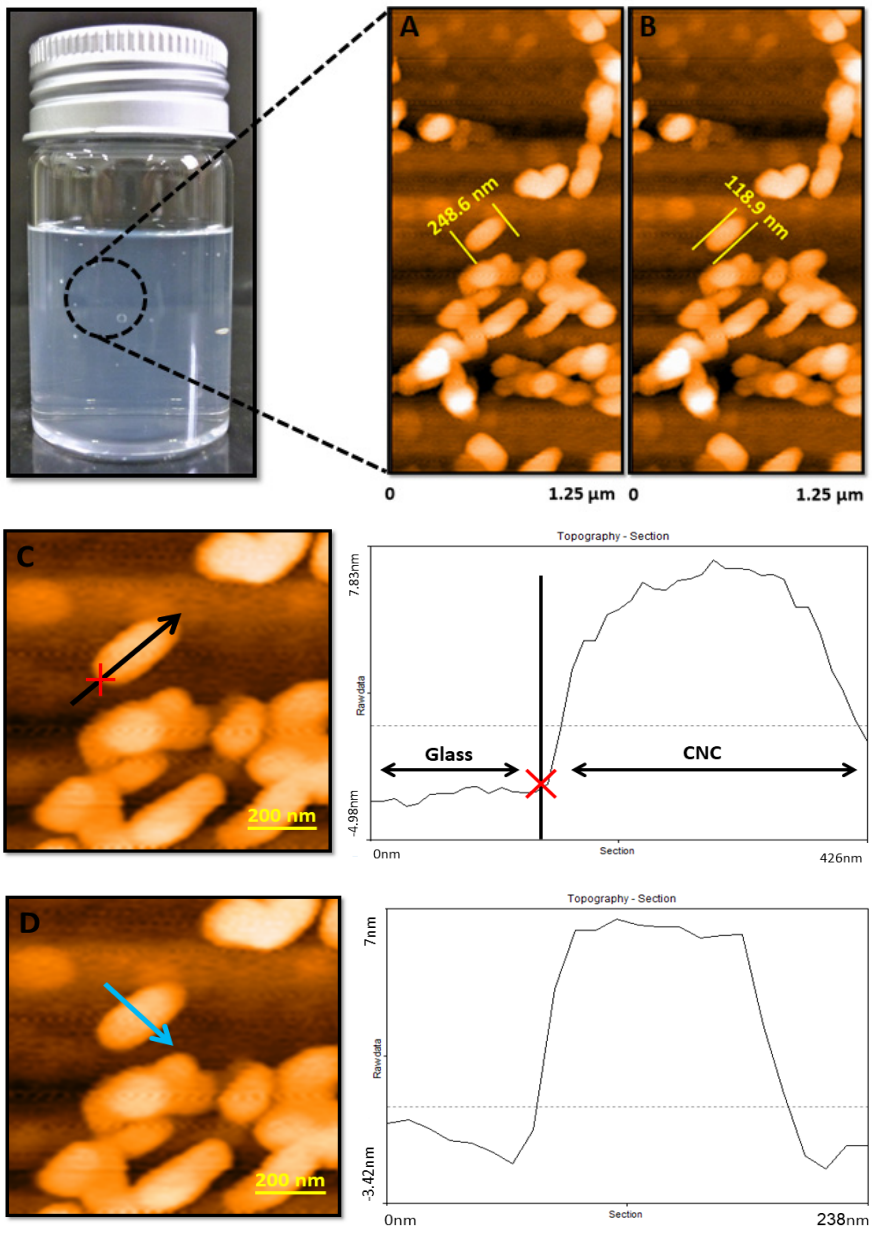

Fig. 6. A) Length of an individual CNC, B) Width of CNC, C) longitudinal cross-section, D) transverse cross-section.

Candanedo et al. [46], but it wasn't done in the present study. Different substrates like glass, silicon, and mica can be used for CNC deposition and affect the final shape and size of CNCs in AFM image. Orue et al. [34] used glass substrate and deposited CNC by spin coating. Fresh cleaved mica is the frequently used substrate for CNC film preparation [41, 42, 51-53]. The type of substrate that is used to prepare the AFM sample, can affect CNC length measurements [47]. The mode of AFM operation is also important. Tapping mode is one of the most utilized modes for CNC detection by AFM [54-56], but the AFM analysis was performed with non-contact mode in the present study. It is also worth mentioning that compression of the CNCs by the AFM tip in contact mode might reduce the apparent CNC height [16]. Tip contamination can affect imaging with AFM [57], too. So it was

better to test a clean glass substrate without any CNC coating to prove tip cleanliness.

Various software are used for size analysis of CNCs like Gwyddion [40], Image J [58], and WS×M [51] (Table 1). Moreover, the selection of analyzable particles (individual CNCs) is somewhat subjective, and different analysts may select and analyze a slightly different subset of particles, resulting in differences in the average height and/or length of the particles. On the other hand, it may be difficult to recognize two particles that are hydrogen-bonded laterally from single CNCs, so it causes heterogeneity in measured widths/heights [42]. The high polydispersity and irregular rod-shape of CNCs are problematic for dimension study [59]. Some researchers use TEM to determine the size of CNCs as seen in Table 1, but TEM has poor contrast and the edge of particles is not clear in TEM, so it may cause overestimation of the CNC dimensions. Thus AFM is more appropriate to determine the size of CNCs in comparison with TEM but it has some limitations, too. For example, the CNCs that comprised of two laterally aggregated primary crystallites appear as single particles and can't be differentiated either by AFM or TEM. The crystallites may be accompanied by amorphous cellulose that was not dissolved during the acid hydrolysis [14, 16], but it can't be distinguished by AFM.

Unfortunately, aggregation and accumulation cannot be avoided in the samples prepared for AFM measurements [9], and they are observable in Fig.s 2 and 3. Hydrogen bonds between crystals make them susceptible to agglomeration. Hydroxyl groups favor the intermolecular hydrogen bond between CNCs. Self-aggregation of CNCs in the casting process can affect precise size analysis. Deposition of CNCs by spin coating can minimize clustering for AFM imaging [16], but this technique can waste the material, too. In this study, many small-size CNCs were ignored during size measurement because of aggregation. Only distinguishable and isolated CNCs were measured. Agglomerated particles and those that touched the edge of the image were excluded during size analysis. Although, three other CNC films were prepared for size measurement in this study, but the numbers of individual CNCs were not sufficient. These primary AFM images can be seen in the supplementary material (Fig. S1).

CNC suspension has an annular pattern during drying originates from capillary flow, because evaporation rates are different across the droplet. Evaporation flux at the edge of the droplet is faster than the center, so the liquid and particles flow to the drop perimeter, and deposition of particles at the edge will increase. This effect causes the arrangement of the nanocrystals during water evaporation and also additional linear dichroism at the edge of the solid film [60].

According to Gray et al. [55], the orientation of CNCs is random below the critical concentration for liquid crystal formation. The ordering phenomenon is probably slower than the evaporation, or gelation occurs below the critical concentration for liquid crystal formation [55]. In the present study, both random and parallel orientation can be seen in Fig.s 2 and 3. Individual CNCs have random orientation, and agglomerated CNCs have approximately orientation along the length. Gray et al. [55] observed that CNCs are fairly uniformly oriented parallel to the edge of the sample in amplitude mode image. Similarly, it is somewhat observable in Fig. 3. The anisotropic orientation of the CNC in the film is the cause of this phenomenon [55]. Chiral nematic phase is also expected for CNCs (Fig. 2). CNCs have cholesteric nematic ordering in aqueous suspension and it can be maintained upon drying [61]. Two factors play a role in the self-assembly process: the first is water evaporation from the anisotropic phase and the second are interactions among particles in the thin film. During water evaporation, the interparticle forces increase and CNCs with different aspect ratios are transferred to different regions of the suspension [60, 62]. Different sides of the CNCs have specific affinities, too [63]. It is supposed that the CNCs with the highest anisotropy assemble at the edge of the solution where the radial flow induces CNC alignment that competes with helical layer formation [60]. The broad distribution of particle length result in the formation of different domains while also contributing to the CNC concentration and thickness gradient toward the edge [62]. So, the accumulation of CNCs at the edge of AFM image in this study can be due to the polydispersity of CNCs in length and aspect ratio (Fig. 2).

The most-reported shape of CNCs is needle-like [38, 64, 65], but they were more ellipsoidal in this work (Fig. 7). This can be justified mostly by the large width of each particle. The maximum width of CNCs is about 70 nm in the literature [11, 66] and it is calculated 138.80 ± 19.64 nm in this

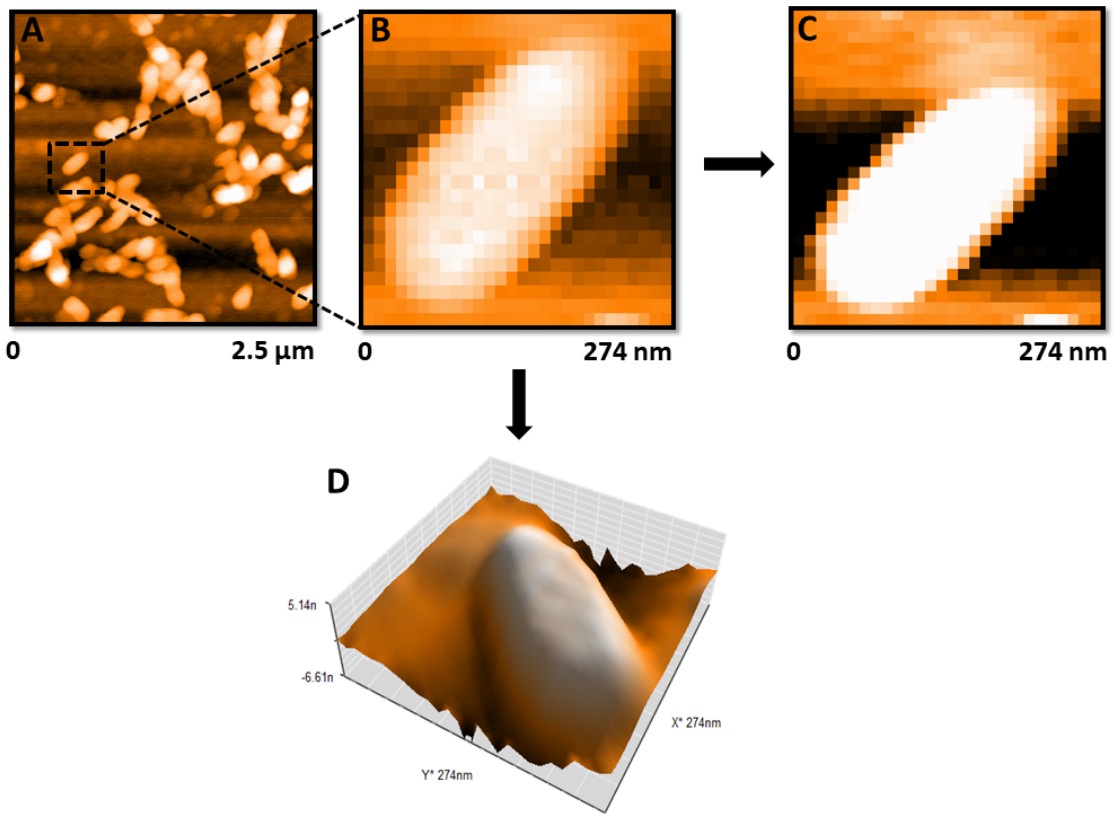

Fig. 7. A) AFM topography polynomial fit image of CNCs, B) topography mean fit image of an individual CNC, C) image of CNC with decreased range of chart data shows the ellipsoidal shape of CNC, D) 3D view of CNC

research, so it would be an overestimation and not reliable. Navarro [14] found that the particle width data are more strongly affected by both AFM tip broadening and the degree of dispersion of the particles than the length data. He also mentioned that AFM thickness measurements are not affected by tip broadening [14]. TEM and AFM are often used for CNC width measurements [67], but both techniques have limitations. The difficulty of selecting single particles for analysis and possible bias due to selection of a specific particle size during sample deposition are the main limitations associated with the microscopy measurements [13]. CNC agglomeration/aggregation has so far been difficult to avoid for CNC samples deposited for microscopy [16], and there is not any guarantee that the sampled images represent the whole nanocellulose sample [67]. Application of proper substrate such as mica and method of deposition like spin coating may decrease this weakness of microscopy. To give accurate results, microscopy-based methods need careful specimen preparation so that specimens contain a representative sample of the particle population and the particles are well separated on the substrate. AFM-based length, width, and thickness values depend highly on the sample preparation [14].

The size of CNC controls its behavior for application such as additive to increase the mechanical strength of composite [9]. Morphology and size of CNCs affect the phase separation behavior and also liquid crystal formation [10]. Size distributions of nanocelluloses are key factors in application to high-strength and light-weight composites [67]. Controlling and measuring the particle size is also critical for assessing the environmental health and safety aspects of nanomaterials, too [9]. Thus it is important to find a standard approach for size study of CNCs.

In general, dimension study is challenging for rod shape nanoparticles like CNCs, especially the width of nano-rods. We tried to explain some possible factors that could affect CNC size. We can't rule out the effect of hydrolysis details on produced CNCs completely, but hydrolysis couldn't be insufficient, either. Because the

produced CNCs were rod shaped. Besides, the average height of the CNCs was consistent with previous studies. Moreover, the mean length of produced CNCs is in a reasonable and acceptable range, although it is slightly larger than some of previous works. But, the overestimation of CNCs' width is most likely due to AFM tip. Although, we didn't test any substrate without CNC deposition to be sure about tip cleanliness, but we couldn't ignore tip ageing, either. The borders of CNCs are exaggerated as seen in Fig. 6. The borders have poor contrast and resolution. It means that the AFM tip was not fresh. Both contamination and ageing can multiply the inherent property of AFM tip in broadening effect. As a result, the CNC width will be more affected than the length. Although, AFM tip can affect both the length and width of CNCs, but length is highly affected by hydrolysis parameters. Insufficient hydrolysis makes the CNCs longer because of remaining amorphous parts (Fig. S2). On the other hand, harsh hydrolysis reaction breaks the crystals and CNCs become shorter. Although, the measured length, height and aspect ratio were in acceptable range, but the accumulation and helical structures of CNCs at the edge of AFM image (Fig. 2) could be due to the polydispersity of produced CNCs, or inherent feature of CNCs in forming chiral nematic phase or both of them. This can't be recognized definitely, but it must be searched in future experiments to prove the hydrolysis efficiency. However, in the case of present study, it is more likely due to the chiral nematic phase of CNCs, because these helical structures were not seen in primary AFM images (Fig. S1).

Atomic Force Microscopy has the potential for comprehensive dimension study of CNCs, but its capability for CNC characterization is not fully investigated, yet. It is important to consider all the essential points before CNC imaging by AFM. This tool is not only useful for size characterization, but also the mechanical properties of CNCs, that can be a research line for future studies. We hope that the CNC beginners gain insights and benefit from the procedure and results of this work.

CONCLUSION

CNCs were successfully produced from Whatman #1 filter paper by acid hydrolysis. Size distribution of CNCs was determined by single particle counting via Atomic Force Microscopy. The length and height of the produced CNCs were consistent with the literature but the measured width was not reliable. We discussed the possible factors that could affect the final AFM images and size of the CNCs, but overestimation of CNC width is mainly due to the AFM tip broadening effect. The AFM tip can affect the final shape of CNCs, too. The ellipsoidal shape of CNCs in this research is more likely due to the magnified width of CNCs. Tip ageing can multiply the broadening effect. In spite of AFM tip ageing in this study, the mean height (thickness) of the produced CNCs was still in acceptable range. It shows that AFM tip has minimum effect on the height of CNCs. On the other hand, the length of CNC can be greatly affected by hydrolysis conditions. As the length of CNCs was in a reasonable range, so we could somehow rule out the hydrolysis insufficiency in this study. The height (thickness) of the CNCs via AFM is the most reliable dimension in the literature in comparison with length and width and it was proved in this research. AFM analysis of the CNCs and the final measured dimensions depend on many factors such as cellulose source, hydrolysis parameters, type of substrate for CNC deposition, method of coating substrate with CNC, sharpness & cleanliness of the AFM tip, tip radius, mode of AFM operation (contact/non-contact), AFM apparatus adjustment, size measurement technique, and analysis software. Several CNC film samples must be prepared for AFM analysis to obtain the size of CNCs more accurate. It is recommended to apply the very sharp, fresh and clean tips with minimum radius to detect and measure CNCs more precisely by AFM. The edge of CNC must be very clear with appropriate resolution for size measurement. AFM with tapping mode is preferred for size analysis and mica is suitable for CNC deposition. More than one analyst should measure individual CNCs to estimate the final size more reliable, thus the analyst bias would be reduced. It is also worthy to create and introduce a standard measurement technique for rod shape nanoparticles to reduce measurement errors and variability among researches. Further experiments are required to optimize the dimensional study of CNCs by AFM.

CONFLICT OF INTEREST

The authors declare that there is no conflict of interest regarding the publication of this manuscript.

REFERENCES

1. Wertz Jean-Luc BdO MJ. Cellulose science and technology.

Lausanne: EPFL Press; 2010.
2. SS GJ. Cellulose nanocrystals: synthesis, functional properties, and applications. Nanotechnology, Science and Applications. 2015;8:45-54.
3. Moon RJ MA NJ, Simonsen J, Youngblood J. Cellulose nanomaterials review: structure, properties, and nanocomposites. Chemical Society Reviews. 2011;40:3941-3994.
4. Yang Y CZ ZJ, Wang G, Zhang R, Dingjie S. Preparation and Applications of the Cellulose Nanocrystal. International Journal of Polymer Science. 2019.
5. Grishkewich N MN TJ, Tam KC. Recent advances in the application of cellulose nanocrystals. Current Opinion in colloid & Interface Science. 2017;29:32-45.
6. Trache D HM HM, Thakur VK. Recent progress in cellulose nanocrystals: sources and production. Nanoscale. 2017;9(5):1763-1786.
7. Dura'n N LA SA. Review of cellulose nanocrystals patents: preparation, composites and general applications. Recent Patents on Nanotechnology. 2012;6(1):16-28.
8. Usov I NG AJ, Handschin S, Schutz C, Fall A, Bergstrom L, Mezzenga R. Understanding nanocellulose chirality and structure–properties relationship at the single fibril level. Nature Communications. 2015;6(16).
9. L T. Cellulose Nanocrystals: Particle Size Distribution and Dispersion in Polymer Composites. Ottawa, Canada: University of Ottawa; 2016.
10. Kaushik M FC CG, Putaux JL, Moores A. Transmission Electron Microscopy for the Characterization of Cellulose Nanocrystals. The Transmission Electron Microscope - Theory and Applications, Khan Maaz: IntechOpen. 2015.
11. Liu Zh HM MG, Yang G, Chen J. Preparation and Characterization of Cellulose Nanocrystals from Wheat Straw and Corn Stalk. Journal of Korea TAPPI. 2019;51(2):40-48.
12. Tan XY AHS LC. Preparation of high crystallinity cellulose nanocrystals (CNCs) by ionic liquid solvolysis. Biomass Bioenergy. 2015;81:584-591.
13. Brinkmann A CM CM, Jakubek ZJ, Leng T, Johnston LJ. Correlating Cellulose Nanocrystal Particle Size and Surface Area. Langmuir. 2016;32:6105−6114.
14. F N. Cellulose Nanocrystals: Size Characterization and Controlled Deposition by Inkjet Printing. Blacksburg, Virginia: Virginia Polytechnic Institute and State University; 2010.
15. Albernaz VL JG LC, Silva LP. Cellulose Nanocrystals Obtained from Rice By-Products and Their Binding Potential to Metallic Ions. Journal of Nanomaterials. 2015.
16. Chen M PJ MA, Couillard M, Zou S, Hackley VA, Johnston LJ. Characterization of size and aggregation for cellulose nanocrystal dispersions separated by asymmetrical-flow field-flow fractionation. Cellulose (Lond). 2019;27(4).
17. Feng. Improving homogeneity of iridescent cellulose nanocrystal films by surfactant assisted spreading self-assembly. ACS Sustainable Chemistry & Engineering. 2019;7(23):19062-19071.
18. H W. Cellulose nanocrystals: properties, production, and applications. Chichester: John Wiley & Sons; 2017.
19. HY LP. Preparation and properties of cellulose nanocrystal: Rods, spheres, and network. Carbohydr Polym. 2010;82:329-336.
20. Hynninen V MP WW, Hietala S, Linder MB, Ikkala O, Nonappa. Methyl cellulose/cellulose nanocrystal nanocomposite fibers with high ductility. Eur Polym J. 2019;112:34-45.
21. Ivanova A F-PB PA, Wagner T, Jumabekov AN, Vilk Y, Weber J, Gunne J, Vignolini S, Tiemann M, Fattakhova-Rohlfing D, Bein T. Cellulose nanocrystal-templated tin dioxide thin film for gas sensing. ACS Applied Materials & Interfaces. 2020;12(11):12639-12647.
22. Li W JB ZS. Preparation of cysteamine-modified cellulose nanocrystal adsorbent for removal of mercury ions from aqueous solutions. Cellu. 2019;26:4971-4985.
23. Maturavongsadit P PG SR, Benhabbour SR. Thermo-/pH-Responsive Chitosan-Cellulose Nanocrystal Based Hydrogel with Tunable Mechanical Properties for Tissue Regeneration Applications. Materialia. 2020;12.
24. Or T SS EA, Osorio DA, De France KJ, Vapaavuori J, Hoare T, Cerf A, Cranston ED, Moran-Mirabal JM. Patterned cellulose nanocrystal aerogel films with tunable dimensions and morphologies as ultra-porous scaffolds for cell culture. ACS Applied Nano Materials. 2019;2(7):4169-4179.
25. Wang J PT XZ, Nigmatullin R, Harniman RL, Eichhorn SJ. Cellulose nanocrystal-polyetherimide hybrid nanofibrous interleaves for enhanced interlaminar fracture toughness of carbon fibre/epoxy composites. Composites Science and Technology. 2019;182.
26. Y J. MANUFACTURING OF NANOCRYSTALLINE CELLULOSE. Espoo, Finland: Aalto University; 2017.
27. Zhao TH PR WC, Lim KTP, Frka-Petesic B, Vignolini S. Printing of responsive photonic cellulose nanocrystal microfilm arrays. Adv Funct Mater. 2019;29(21).
28. Olivier C MC BP, Bizot H, Chauvet O and Cathala B. Cellulose nanocrystal-assisted dispersion of luminescent single-walled carbon nanotubes for layer-by-layer assembled hybrid thin films. Langmuir. 2012;28:12463-12471.
29. Urena-Benavides EE BP KC. Effect of jet stretch and particle load on cellulose nanocrystal-alginate nanocomposite fibers. Langmuir. 2010;26(17):14263-14270.
30. Bushell M MJ CM, Batchelor W, Browne C, Cho JY, et al. Particle size distributions for cellulose nanocrystals measured by atomic force microscopy: an interlaboratory comparison. Cellu. 2021;28:1387-1403.
31. TJ DA-L. Cellulose degradation in an acetic acid environment. Studies in Conservation. 2000;45(3):201-210.
32. Abushammala H KI LM. Ionic-mediated technology to produce cellulose nanocrystals directly from wood. Carbohydr Polym. 2015;134:609-616.
33. Wu Q MY WS, Li Y, Fu S, Ma L, Harper D. Rheological behavior of cellulose nanocrystal suspension: influence of concentration and aspect ratio. J Appl Polym Sci. 2014;131(15).
34. Orue A S-EA EA, Pena-Rodriguez C. Office waste paper as cellulose nanocrystal source. J Appl Polym Sci. 2017;134(35).
35. Sadeghifar H FI, Clarke SP, Brougham DF, Argyropoulos DS. Production of cellulose nanocrystals using hydrobromic acid and click reactions on their surface. JMatS. 2011;46:7344-7355.
36. Pakzad A SJ HPaYR. Size effects on the mechanical properties of cellulose I nanocrystals. Journal of Materials Research. 2012;27(3):528-536.
37. Annamalai PK DK MS, Foster EJ, Rowan SJ and Weder C. Water-resposive mechanically adaptive nanocomposites based on styrene-butadiene rubber and cellulose

nanocrystals-processing matters. ACS Applied Materials & Interfaces. 2014;6(2):967-976.
38. Rahimi Kord sofla M BR TT, Rainey T. A comparison of cellulose nanocrystals and cellulose nanofibers extracted from bagasse using acid and ball milling methods. Advances in Natural Sciences: Nanoscience and Nanotechnology. 2016;7(3):1-9.
39. Li MC WQ SK, Lee S, Qing Y and Wu Y. Cellulose nanoparticles: Structure-Morphology-Rheology relationship. ACS Sustainable Chemistry & Engineering. 2015;3(5):821-832.
40. Brito BSL PF PJ, Jean B. Preparation, morphology and structure of cellulose nanocrystals from babmboo fibers. Cellu. 2012;19:1527-1536.
41. Wu Q MY CK, Wang S, Li Y, Ma L, Fu S. Influence of temperature and humidity on nano-mechanical properties of cellulose nanocrystal films made from switchgrass and cotton. Industrial Crops and Products. 2013;48:28-35.
42. Jakubek ZJ CM CM, Leng T, Liu L, Zou S, Baxa U, Clogston JD, Hamad WY, Johnston LJ. Characterization challenges for a cellulose nanocrystal reference material: dispersion and particle size distributions. Journal of Nanoparticle Research. 2018;20.
43. Blanco A MM CC, Balea A, Merayo N, Negro C. Handbook of nanomaterials for industrial applications. Amsterdam: Elsevier Inc; 2018.
44. Sinha A ME LK, Carrier DJ, Han H, Zharov VP, Kim JW. Cellulose nanocrystals as advanced “green” materials for biological and biomedical engineering. Journal of Biosystems Engineering. 2015;40(4):373-393.
45. YJ YY, inventorFunctionalized cellulose nanocrystal materials and methods of preparation2017.
46. Beck-Candanedo S RM GD. Effect of Reaction Conditions on the Properties and Behavior of Wood Cellulose Nanocrystal Suspensions. Biomacromolecules. 2005;6(2):1048-1054.
47. VT KE. Indirect evidence of supramolecular changes within cellulose microfibrils of chemical pulp fibers upon drying. Cellu. 2009;16:65-74.
48. Tian C ZL MQ, Cao C, Ni Y. Improving the reactivity of kraft-based dissolving pulp for viscose rayon production by mechanical treatments. Cellu. 2014;21:3647-3654.
49. Gicequel E BJ RC, Putaux JL, Pignon F, Jean B and Martin C. Impact of sonication on the rheological and colloidal properties of highly concentrated cellulose nanocrystal suspensions. Cellu. 2019;26:7619-7634.
50. Da Silva ISV NW SH, Pasquini D, Andrade MZ, Otaguro H. Mechanical, thermal and barrier properties of pectin/cellulose nanocrystal nanocomposite films and their effect on the storability of strawberries (fragaria ananassa). Polym Adv Technol. 2015;28(8):1005-1012.
51. Lahiji RR XX RR, Raman A, Rudie A, Moon RJ. Atomic force microscopy characterization of cellulose nanocrystals. Langmuir. 2010;26(6):4480-4488.
52. Meng Y WQ YT, Huang B, Wang S, Li Y. Analyzing three-dimentional structure and geometrical shape of individual cellulose nanocrystal from switchgrass. Polymer composites. 2015;38(11):2368-2377.
53. Li X LJ GJ, Kuang Y, Mo L, Song T. Cellulose nanocrystals (CNCs) with different crystalline allomorph for oil in water Pickering emulsions. Carbohydr Polym. 2018;183:303-310.
54. KM KV. Effect of drying conditions on cellulose nanocrystal (cnc) agglomerate porosity and dispersibility in polymer nanocomposites. Powder Technol. 2014;261:288-298.
55. MX GD. Chiral nematic structure of cellulose nanocrystal suspensions and films; Polarized light and atomic force microscopy. Materials. 2015;8(11):7873-7888.
56. Saralegi A RL ML, Arbelaiz A, Eceiza A, Corcuera MA. From elastomeric to rigid polyurethane/cellulose nanocrystal bionanocomposites. Composites Science and Technology. 2013;88:39-47.
57. GD LJ. AFM of adsorbed polyelectrolytes on cellulose I surfaces spin-coated on silicon wafers. Cellu. 2005;12:127-134.
58. Neto WPF PJ MM, Ogawa Y, Harumi O, Pasquini D, Dufresne A. Comprehensive morphological and structural investigation of cellulose I and II nanocrystals prepared by sulfuric acid hydrolysis. RSC Advances. 2016;6(79):76017-76027.
59. Chen JH LJ SY, Xu ZH, Li MC, Ying RF, Wu JQ. Preparation and properties of microfibrillated cellulose with different carboxyethyl content. Carbohydr Polym. 2019;206:616-624.
60. Dumanli AG KH KG, Reisner E, Baumberg JJ, Steiner U, Vignolini S. Digital color in cellulose nanocrystal films. ACS Applied Materials & Interfaces. 2014;6(15):12302-12306.
61. Marchessault RH MF WN. Liquid crystal systems from fibrillar polysaccharides. Nature. 1959;184:632-633.
62. O L. The effects of shape on the interaction of colloidal particles. Annals of the NewYork Academy of Sciences. 1949;51(4):627-659.
63. Cherhal F CF CI. Influence of charge density and Ionic strength on the aggregation process of cellulose nanocrystals in aqueous suspension, as revealed by small-angle neutron scattering. Langmuir. 2015;31(20):5596-5602.
64. Huang S ZL LM, Wu Q, Kojima Y, Zhou D. Preparation and properties of electrospun Poly(Vinyl Pyrrolidone)/Cellulose nanocrystal /silver nanoparticle composite fibers. Materials. 2016;9(7).
65. Taipina MDO FM YI, Goncalves MDC. Surface modification of cotton nanocrystals with a silane agent. Cellu. 2013;20:217-226.
66. He M LY, Won JM. Effect of the modification of PCC with NCC on the paper properties. Journal of Korea TAPPI. 2015;47(4):136-143.
67. A I. Determination of length and width of nanocelluloses from their dilute dispersions. In Advances in Pulp and Paper Research, 16th Fundamental Research Symposium; OXFORD, ; Manchester2017. p. 801-811.